

#### Anonymous Referee #1

This work presents the results of the field measurement of air pollution during 2019 Spring Festival. Spring Festival is a special period to investigate the impact of emission reduction on air quality. The topic itself is very interesting. The authors provide very interesting data. However, there's a major defect for the current manuscript. The authors compared the variation of various air pollutants, and gave the conclusion that the reduction of "Sharply reduced sulfur dioxide (SO<sub>2</sub>) and nitrogen dioxide (NO<sub>2</sub>) concentrations during the festival holiday resulted in an unexpected increase in the surface ozone (O<sub>3</sub>) concentration", and further promote the secondary formation. These conclusions are astonishing and new, but the authors did not provide enough convincing evidence. Besides, considering the quality of ACP, I will not recommend the publication of this manuscript.

**Response:** While we appreciate the critical comment of the review, it'd be much more helpful if the reviewer could have provided a more informative and insightful comment so that we know more about his/her concern. For any scientific research, a finding of "astonishing and new" should not be the reason for rejection.

In this study, we investigated the impact of emission reductions on the concentrations of several trace gases and their further impact on aerosol formation during the special period of the 2019 Spring Festival. It is clear that emission reductions could efficiently reduce primary pollutants (SO<sub>2</sub>, NO<sub>x</sub>, BC, etc.). The time series of O<sub>x</sub> (O<sub>3</sub>+NO<sub>2</sub>) added in Fig. 2 depicts a weak decrease of O<sub>x</sub> from the POL period to the BG period, suggesting that the possible appeared O<sub>3</sub>-titration made [O<sub>3</sub>] increase during the BG period. Simultaneously, the mass concentrations of secondary inorganics decreased but their reduction percentages were much lower than those of primary pollutants. With the further analysis of SOR, NOR, and their relationships with ambient RH and ALWC, we concluded that the enhancement of aqueous chemical reactions oxidized by the dissolved O<sub>3</sub> maybe the main reason causing the enhanced secondary inorganic aerosol (SIA) formation, especially for sulfate.

In recent years, the annual average PM<sub>2.5</sub> concentration has decreased rapidly in China, benefitting from the implementation of many emission reduction measures taken by the Chinese government. However, the mass fraction of inorganics increased by more than 10 % during these years (H. Li et al., 2019; Y. Wang et al., 2019), implying the formation enhancement of secondary inorganic aerosols (SIA), which partly counteracted the decrease in PM<sub>2.5</sub>. Xie et al. (2020) found that the aerosol pH level increased as PM<sub>2.5</sub> decreased in urban Beijing because of the increased mass ratio of nitrate to sulfate. They also stated that the major chemical processes during haze events and the control target should be re-evaluated to obtain the most effective control strategy. As one possible consequence of the increased aerosol pH, the dissolved O<sub>3</sub> in particles may play a more important role in SIA formation, especially for sulfate (Seinfeld and Pandis, 2016). Our study provides sound evidence for this.

Other recent studies have also suggested that the role of O<sub>3</sub> on SIA formation cannot be neglected. For example, Fang et al. (2019) found that relative humidity (RH) and O<sub>3</sub> concentration were two important prerequisites for sulfate formation, based on a year-long set of field measurements made in Beijing. They found a rapid rise in the SOR at the RH

threshold of ~ 45% or an O<sub>3</sub> concentration threshold of ~35 ppb, similar to what we found in our study. As another example, Huang et al. (2020) investigated air quality during the COVID-19 lockdown using comprehensive measurements and modeling with a focus on China. They also found that a large reduction in emissions could enhance the concentration of O<sub>3</sub> in winter in the Beijing-Tianjin-Hebei (BTH) region, promoting SIA formation through the enhancement of nocturnal aqueous chemical reactions during the COVID-19 lockdown.

## References

- Fang, Y., Ye, C., Wang, J., Wu, Y., Hu, M., Lin, W., Xu, F., and Zhu, T.: Relative humidity and O<sub>3</sub> concentration as two prerequisites for sulfate formation, *Atmos. Chem. Phys.*, 19, 12,295–12,307, <https://doi.org/10.5194/acp-19-12295-2019>, 2019.
- Huang, X., Ding, A., Gao, J., Zheng, B., Zhou, D., Qi, X., Tang, R., Wang, J., Ren, C., Nie, W., Chi, X., Xu, Z., Chen, L., Li, Y., Che, F., Pang, N., Wang, H., Tong, D., Qin, W., Cheng, W., Liu, W., Fu, Q., Liu, B., Chai, F., Davis, S. J., Zhang, Q., and He, K.: Enhanced secondary pollution offset reduction of primary emissions during COVID-19 lockdown in China, *National Science Review*, <https://doi.org/10.1093/nsr/nwaa137>, 2020.
- Li, H., Cheng, J., Zhang, Q., Zheng, B., Zhang, Y., Zheng, G., and He, K.: Rapid transition in winter aerosol composition in Beijing from 2014 to 2017: response to clean air actions, *Atmos. Chem. Phys.*, 19, 11,485–11,499, <https://doi.org/10.5194/acp-19-11485-2019>, 2019.
- Seinfeld, J. H., and Pandis, S. N.: *Atmospheric chemistry and physics: from air pollution to climate change*, edited, John Wiley & Sons, 2016.
- Wang, Y., Chen, J., Wang, Q., Qin, Q., Ye, J., Han, Y., Li, L., Zhen, W., Zhi, Q., Zhang, Y., and Cao, J.: Increased secondary aerosol contribution and possible processing on polluted winter days in China, *Environ. Int.*, 127, 78–84, <https://doi.org/10.1016/j.envint.2019.03.021>, 2019.
- Xie, Y., Wang, G., Wang, X., Chen, J., Chen, Y., Tang, G., Wang, L., Ge, S., Xue, G., Wang, Y., and Gao, J.: Nitrate-dominated PM<sub>2.5</sub> and elevation of particle pH observed in urban Beijing during the winter of 2017, *Atmos. Chem. Phys.*, 20, 5019–5033, <https://doi.org/10.5194/acp-20-5019-2020>, 2020.

## Anonymous Referee #2

Comments on manuscript entitled "Enhancement of secondary aerosol formation by reduced anthropogenic emissions during Spring Festival 2019 and enlightenment for regional PM<sub>2.5</sub> control in Beijing"

General comments: This manuscript reported primary pollutant reduction but enhanced SIA formation in an emission reduction period during the 2019 Spring Festival in Beijing. The opposite trend of atmospheric oxidative capacity responding emission reduction was proposed the cause for enhanced SIA formation. Though the supporting discussion still appeared to be weak. Nevertheless, this study should call for the attention on SIA pollution control policy mitigation. I thus recommend publication of this manuscript on ACP with minor revision.

Specific comments:

Lines 21-22: O<sub>3</sub> control regime on a regional scale is still a controversial topic. This manuscript did not intend to discuss on such topic given no VOCs measurements were present. Therefore, it is a bit risky to go such far with current data available. I suggest to delete the statement on NO<sub>x</sub> and VOCs control strategy if no more discussion shall add.

**Response:** Agreed. The sentence "The emission control of volatile organic compounds (VOCs) may be more suitable than the emission control of NO<sub>x</sub> to reduce O<sub>3</sub> because VOCs under current emission conditions likely control the formation of O<sub>3</sub> in winter in the BTH region" has been deleted.

Line 56: be specific! Change to "secondary inorganic aerosol formation"

**Response:** Revised.

Line 92: consider to revise this sentence

**Response:** This sentence has been revised as: "Our measurements around this period of the field campaign are thus ideal for investigating the impact of reduced anthropogenic emissions on surface O<sub>3</sub> and aerosol formation."

Line 160: as shown in Fig.2, O<sub>3</sub> titration appeared to occur in both POL and BG period. O<sub>x</sub>=O<sub>3</sub>+NO<sub>2</sub> is thus suggested to add in Fig.2.

**Response:** The time series of O<sub>x</sub> (O<sub>3</sub>+NO<sub>2</sub>) has been added to Fig. 2 in the manuscript (shown below as Fig. R1). It shows a weak variation of O<sub>x</sub> from the POL period to the BG period, indicating that the presence of strong O<sub>3</sub>-titration during Spring Festival 2019. The corresponding discussion about O<sub>x</sub> and O<sub>3</sub> titration has been added to section 3.1 of the revised manuscript.

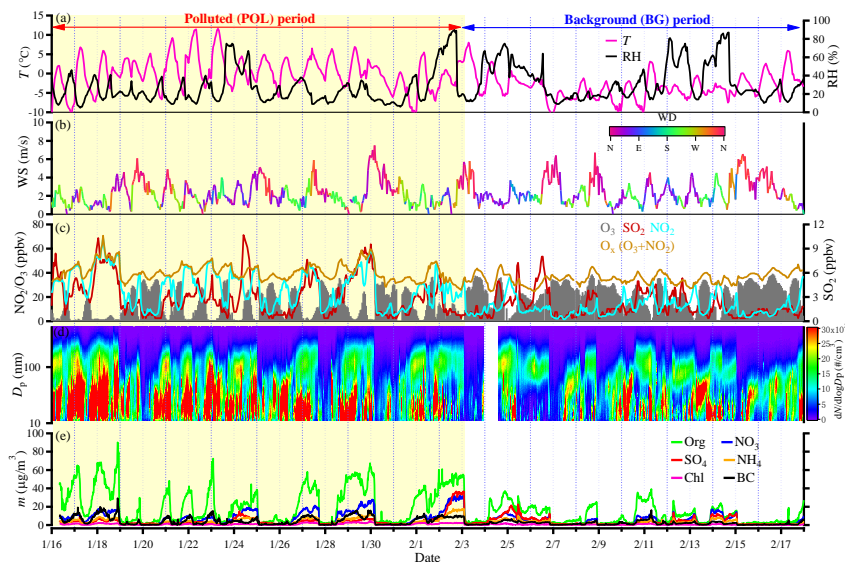


Figure R1. Time series of (a) ambient temperature ( $T$ ) and relative humidity (RH), (b) wind direction (WD) and speed (WS), (c) volume mixing ratios of trace gases [ $O_3$ ,  $SO_2$ ,  $NO_2$  and  $O_x$  ( $O_3+NO_2$ )], (d) the aerosol particle number size distribution measured by the SMPS, and (e) mass concentrations of aerosol chemical species in  $PM_{2.5}$  measured by the ACSM and the AE-33. The trace gas information was from the Yizhuang station, and the others were observed at the experiment site in Beijing (16 January to 17 February 2019).

Lines 202-203: cannot read from Figure 2 that  $m_{org}$  and  $m_{BC}$  increase by % at night from daytime is less in BG relative to POL Lines

**Response:** We're sorry that this sentence has confused the reviewer. Figure 2e depicts that the peaks of  $m_{org}$  and  $m_{BC}$  at night during the BG period were much lower than those during the POL period, caused by emission reductions during the BG period. Therefore, here we want to express that the enhancement of  $m_{org}$  and  $m_{BC}$  at night during the BG period was not as strong as that during the POL period.

This sentence has been revised as: "However, the increases in  $m_{org}$  and  $m_{BC}$  at night during the BG period were not as strong as those during the POL period."

203-204: both  $m_{nitrate}$  and  $m_{sulfate}$  varied!

**Response:** Figure 2e depicts that both  $m_{NO_3}$  and  $m_{SO_4}$  decreased from the POL period to the BG period. However, their reduction magnitudes differed considerably.

Lines 246-24: decreased from what?

**Response:** This sentence has been revised as: "Table 2 also indicates that the mass concentrations ( $m$ ) of aerosol chemical species in  $PM_{2.5}$  were much less during the BG period than during the POL period".



Lines 255-257: From the context, I can only get that Org and BC reduction was sharper than sulfate and nitrate. If I can accept that “secondary (inorganic) aerosol” could replace “sulfate and nitrate”, I am still reluctant to accept that Org and BC are all primary aerosol.

**Response:** The reviewer asks a good question. BC is mainly from primary emissions, but organics were not. Part of the organics is from primary emissions (i.e., primary organic aerosols, or POA), but another part is from gas-to-particle transformations (i.e., secondary organic aerosols, or SOA). Unfortunately, we are not able to separate POA and SOA in organics using our measurement data from the campaign. In this paper, we were not trying to define BC and organics as the primary matter. They were simply regarded as representing primary matter because many of them were from primary emissions. To a certain extent, the mass variations of BC and organics can represent the mass variations of primary aerosols. Similarly, SIA matter (mainly sulfate, nitrate and ammonium) are important chemical components of secondary aerosols, so their mass variations can represent the mass variations of secondary aerosols.

Figure 5: The high SIA and large PM<sub>2.5</sub> number in POL were mostly seen at low RH, which is against the impression that heavy PM<sub>2.5</sub> pollution was usually accompanied by high RH condition in literature. The author should at least address such unusual data.

**Response:** Some studies have found that heavy haze events are generally associated with high RH conditions and southerly winds. This is because the southerly winds are not only beneficial to the transport of pollutants from southern highly industrialized areas, but also to the transport of water vapor. In our study, the prevailing winds during both the POL and BG periods were northerly, which were beneficial to dispersing pollutants in Beijing, so no heavy haze episodes occurred during the two periods. However, the PM<sub>2.5</sub> during the POL period with ordinary emission conditions could reach moderate pollution level (over 100  $\mu\text{g}/\text{m}^3$ ) although the ambient RH was low.

The basic meteorological and environmental characteristics have been described in section 3.1.

Figure 6: Given the discussion on RH or ALWC in the context, I would suggest to add one of the two parameters in one column.

**Response:** That is a good suggestion. A figure showing the diurnal variation in ambient relative humidity (RH) (Fig. R2 below) was added to the supplement (Fig. S4). It shows that the ambient RH levels at night are elevated during both the POL and BG periods, favorable for aqueous chemical reactions.

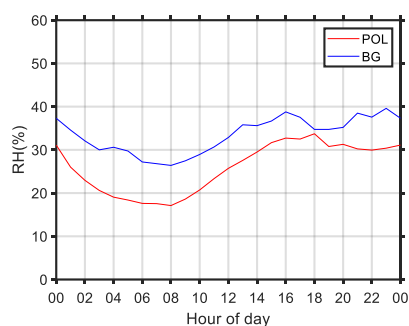


Figure R2. Diurnal variation of ambient relative humidity (RH) during the POL and BG periods.

Line 403: High O<sub>3</sub> concentration itself will not surely lead to strong atmospheric oxidative capacity or even O<sub>3</sub> production. The first reason is that O<sub>3</sub> was titrated in Figure 2. The secondary reason is that O<sub>3</sub> can be regionally transported as a relatively long-lived species. And the third, OH instead of O<sub>3</sub> is the major oxidant in the atmosphere, which better represents the atmospheric oxidative capacity and does not differ significantly from pollution days to clean days in winter Beijing (see Eloise et al., Elevated levels of OH observed in haze events during wintertime in central Beijing). More data or discussion are needed here.

**Response:** Agreed. The analysis of O<sub>x</sub> above shows that O<sub>3</sub>-titration appeared during the special period studied. In this campaign, OH was not measured, so the atmospheric oxidation capacity wasn't analyzed accurately. For this reason, the discussion about atmospheric oxidation capacity in the manuscript has been deleted.

**Enhancement of secondary aerosol formation by reduced anthropogenic emissions during Spring Festival 2019 and enlightenment for regional PM<sub>2.5</sub> control in Beijing**

Yuying Wang<sup>1</sup>, Zhanqing Li<sup>2</sup>, Qiuyan Wang<sup>1</sup>, Xiaoai Jin<sup>3</sup>, Peng Yan<sup>4</sup>, Maureen Cribb<sup>2</sup>, Yanan Li<sup>4</sup>, Cheng Yuan<sup>1</sup>, Hao Wu<sup>3</sup>, Tong Wu<sup>3</sup>, Rongmin Ren<sup>3</sup>, Zhaoxin Cai<sup>3</sup>

<sup>1</sup>Key Laboratory for Aerosol-Cloud-Precipitation of China Meteorological Administration, School of Atmospheric Physics, Nanjing University of Information Science & Technology, Nanjing 210044, China

<sup>2</sup>Earth System Science Interdisciplinary Center, Department of Atmospheric and Oceanic Science, University of Maryland, College Park, MD, USA

<sup>3</sup>State Key Laboratory of Remote Sensing Science, College of Global Change and Earth System Science, Beijing Normal University, Beijing 100875, China

<sup>4</sup>CMA Meteorological Observation Center, Centre for Atmosphere Watch and Services, Beijing 100081, China

Correspondence to: Yuying Wang (yuyingwang@nuist.edu.cn)

## 1 Abstract

2 A comprehensive field experiment measuring aerosol chemical and physical  
3 properties at a suburban site in Beijing around the 2019 Spring Festival was carried out  
4 to investigate the impact of reduced anthropogenic emissions on aerosol formation.  
5 Sharply reduced sulfur dioxide (SO<sub>2</sub>) and nitrogen dioxide (NO<sub>2</sub>) concentrations during  
6 the festival holiday resulted in an unexpected increase in the surface ozone (O<sub>3</sub>)  
7 concentration ~~caused by the strong O<sub>3</sub>-titration phenomenon, leading to enhancement~~  
8 ~~of the atmospheric oxidation capacity~~. Simultaneously, the reduced anthropogenic  
9 emissions resulted in massive decreases in particle number concentration at all sizes  
10 and the mass concentrations of organics and black carbon. However, the mass  
11 concentrations of inorganics (especially sulfate) decreased weakly. Detailed analyses  
12 of the sulfur oxidation ratio and the nitrogen oxidation ratio suggest that sulfate  
13 formation during the holiday could be promoted by enhanced nocturnal aqueous-phase  
14 chemical reactions between SO<sub>2</sub> and O<sub>3</sub> under moderate relative humidity (RH)  
15 conditions (40 % < RH < 80 %). Daytime photochemical reactions in winter in Beijing  
16 mainly controlled nitrate formation, which was enhanced a little during the holiday. A  
17 regional analysis of air pollution patterns shows that the enhanced formation of  
18 secondary aerosols occurred throughout the entire Beijing-Tian-Hebei (BTH) region  
19 during the holiday, partly offsetting the decrease in particle matter with an aerodynamic  
20 diameter less than 2.5 μm. Our results highlight the necessary control of O<sub>3</sub> formation  
21 to reduce secondary pollution in winter ~~under current emission conditions. The~~  
22 ~~emission control of volatile organic compounds (VOCs) may be more suitable than the~~

23 ~~emission control of NO<sub>x</sub> to reduce O<sub>3</sub> because VOCs under current emission conditions~~  
24 ~~likely control the formation of O<sub>3</sub> in winter in the BTH region.~~

## 26 1. Introduction

27 Aerosols consist of liquid and solid particles, and their mixture suspended in the  
28 atmosphere. The massive increase in aerosol particles caused by human activities (~~e.g.,~~  
29 ~~traffic, industrial production, and construction work~~) in urban areas (e.g., traffic,  
30 industrial production, and construction work) can deteriorate air quality to the point of  
31 having a detrimental impact on human health (e.g., Chow et al., 2006; Matus et al.,  
32 2012; Gao et al., 2017; Zhong et al., 2018; An et al., 2019). Moreover, aerosols can  
33 change atmospheric optical and hygroscopic properties, altering the transfer of solar  
34 radiation and the development of clouds, thereby changing weather and climate in both  
35 aerosol source regions and their downstream areas (e.g., Altaratz et al., 2014; R. Zhang  
36 et al., 2015; Z. Li et al., 2016, 2019; Y. Wang et al., 2018, 2019b; Jin et al., 2020).

37 With the rapid economic development and urbanization in recent decades in China,  
38 the scales of many cities have expanded quickly along with sharply increased  
39 populations in urban areas, especially in the three most economically developed regions  
40 (the Beijing-Tianjin-Hebei (BTH) metropolitan region, the Yangtze River Delta, and  
41 the Pearl River Delta). As a result, air pollution has become a severe problem in these  
42 megacity regions (e.g., Chan and Yao, 2008; Han et al., 2014; Zhong et al., 2018). On  
43 some heavy haze days, the mass concentration of particulate matter with an  
44 aerodynamic diameter of less than 2.5  $\mu\text{m}$  (PM<sub>2.5</sub>) dramatically increased from tens to

45 hundreds of micrograms per cubic meter in several hours (Guo et al., 2014; Sun et al.,  
46 2016a).

47 Over the past a few years, many emission control measures have been taken in  
48 China to mitigate air pollution. As a response, the mass concentration of PM<sub>2.5</sub> has  
49 decreased in most cities in China since 2013, especially in the BTH region (Q. Zhang  
50 et al., 2019; Vu et al., 2019; Zhai et al., 2019). Organics and black carbon (BC)  
51 concentrations largely decreased during these years thanks to the reduction in coal  
52 combustion and biomass burning (H. Li et al., 2019a; Xu et al., 2019). Simultaneously,  
53 the mass concentrations of inorganics (mainly sulfate, nitrate, and ammonium) also  
54 decreased due to the reduction in their gaseous precursors (especially sulfur dioxide, or  
55 SO<sub>2</sub>). However, the mass fraction of inorganics increased by more than 10 % during  
56 these years (H. Li et al., 2019a; Y. Wang et al., 2019a), implying the enhancement of  
57 secondary inorganic aerosol (SIA) formation, which partly counteracted the decrease  
58 in PM<sub>2.5</sub>. All these variations would change aerosol physicochemical properties. For  
59 example, Xie et al. (2020) found that the aerosol pH increased as PM<sub>2.5</sub> decreased in the  
60 past few years in urban Beijing due to the enhanced mass ratio of nitrate to sulfate. As  
61 a possible consequence of the elevated aerosol pH, the dissolved ozone (O<sub>3</sub>) in particles  
62 would play a more important role to SIA formation, especially for sulfate formation  
63 (Seinfeld and Pandis, 2016). Therefore, the major chemical processes during haze  
64 events and the control target should be re-evaluated. Therefore, e Elaborating the  
65 secondary aerosol formation mechanism under current emission conditions is important  
66 for taking more proper measures to control PM<sub>2.5</sub> in the future.

- 带格式的: 字体: (默认) Times New Roman, 小四, 字体颜色: 自动设置
- 带格式的: 字体: (默认) Times New Roman, 小四, 字体颜色: 自动设置
- 带格式的: 字体: (默认) Times New Roman, 小四, 字体颜色: 自动设置, 下标
- 带格式的: 字体: (默认) Times New Roman, 小四, 字体颜色: 自动设置
- 带格式的: 字体: (默认) Times New Roman, 小四, 字体颜色: 自动设置
- 带格式的: 字体: (默认) Times New Roman, 小四, 字体颜色: 自动设置
- 带格式的: 字体: (默认) Times New Roman, 小四, 字体颜色: 自动设置
- 带格式的: 字体: (默认) Times New Roman, 小四, 字体颜色: 自动设置
- 带格式的: 字体: (默认) Times New Roman, 小四, 字体颜色: 自动设置
- 带格式的: 字体: (默认) Times New Roman, 小四, 字体颜色: 自动设置
- 带格式的: 字体: (默认) Times New Roman, 小四, 字体颜色: 自动设置
- 带格式的: 字体: (默认) Times New Roman, 小四, 字体颜色: 自动设置
- 带格式的: 字体: (默认) Times New Roman, 小四, 字体颜色: 自动设置
- 带格式的: 字体: (默认) Times New Roman, 小四, 字体颜色: 自动设置
- 带格式的: 字体: (默认) Times New Roman, 小四, 字体颜色: 自动设置
- 带格式的: 字体: (默认) Times New Roman, 小四, 字体颜色: 自动设置
- 带格式的: 字体: (默认) Times New Roman, 小四, 字体颜色: 自动设置

67           Some studies have argued that controlling emissions of nitrogen oxides ( $\text{NO}_x$ ) is  
68 important because nitrate in  $\text{PM}_{2.5}$  has had the weakest decrease relative to other  
69 chemical species over the past several years (Q. Zhang et al., 2019; F. Zhang et al.,  
70 2020). The transformation of  $\text{NO}_x$  to nitrate is closely related to atmospheric oxidation  
71 processes (Seinfeld and Pandis, 2016). Surface ozone ( $\text{O}_3$ ) is an important secondary  
72 gaseous pollutant and oxidizing agent in the atmosphere. Recent studies have found  
73 that a reduction in  $\text{PM}_{2.5}$  resulted in an increase in the  $\text{O}_3$  volume mixing ratio ( $[\text{O}_3]$ ) at  
74 a rate of 3.3 ppbv per annum during the summer of the past few years in the BTH region  
75 (K. Li et al., 2019, 2020). The increased  $[\text{O}_3]$  can enhance the atmospheric oxidation  
76 capacity, thereby promoting the formation of secondary aerosols in summer (T. Wang  
77 et al., 2017). However, less emphasis has been placed on the variation in  $[\text{O}_3]$  in winter.  
78 The formation of  $\text{O}_3$  and its effect on secondary aerosol formation in a cold environment  
79 is thus unclear.

80           Some special events held in China have provided unique opportunities to  
81 investigate the impact of human activities on air quality by taking advantage of unusual  
82 changes associated with short-term, drastic measures implemented by the Chinese  
83 government to reduce anthropogenic emissions, such as the 2008 Summer Olympic  
84 Games (T. Wang et al., 2010; Guo et al., 2013), the 2014 Asia-Pacific Economic  
85 Cooperation (Sun et al., 2016b), the 2015 China Victory Day parade (Y. Wang et al.,  
86 2017; Zhao et al., 2017), and the 2016 G20 Summit (H. Li et al., 2019b). The annual  
87 Spring Festival holiday is also a special occasion when the vast majority of the  
88 population stops working for 2 to 4 weeks (Tan et al., 2009; Y. Zhang et al., 2016; C.

89 Wang et al., 2017). Investigating the impact of changes in anthropogenic emissions on  
90 gaseous pollutants and aerosol formation during these special occasions may provide  
91 useful guidance on more scientifically sound measures to take to control PM<sub>2.5</sub>.

92 A comprehensive aerosol field experiment at a suburban site near the 5th Ring  
93 Road in the Daxing District of Beijing was carried out for more than two years,  
94 including the 2019 Spring Festival. Beijing was one of the three top cities in China with  
95 the largest migrating population during the 2019 Spring Festival holiday  
96 (<https://cloud.tencent.com/developer/news/393324>). In addition, fireworks were  
97 prohibited throughout the Beijing metropolitan region within the 6th Ring of the Beijing  
98 Beltway. The intensity of anthropogenic emissions was thus much weaker than usual  
99 during this holiday. Our measurements ~~made~~ around this period of the field campaign  
100 are thus ideal for investigating the impact of reduced anthropogenic emissions on  
101 surface O<sub>3</sub> and aerosol formation.

102 This paper is structured as follows. Section 2 describes the experiment site and the  
103 measurement data used in this study. Section 3 presents the results and discussion,  
104 mainly concerning the impact of reduced anthropogenic emissions during the holiday  
105 on the variations in trace gases and aerosol chemical species in Beijing and the BTH  
106 region. Section 4 presents the conclusions and their implications.

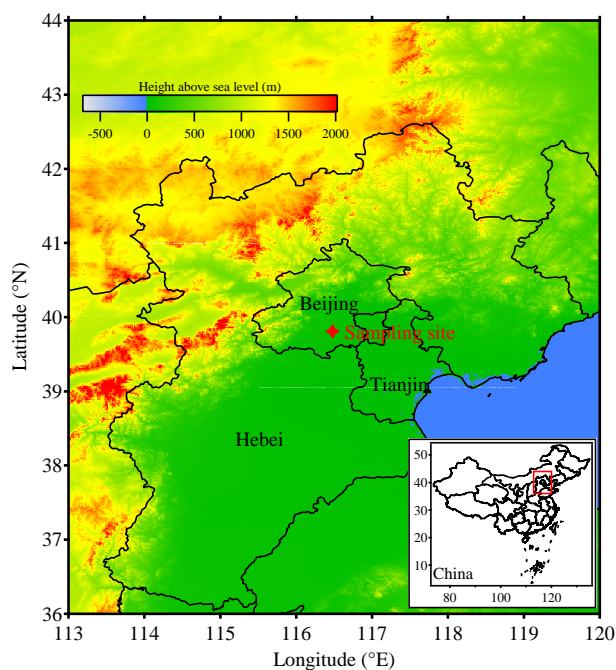
107

## 108 **2. Experiment site and measurement data**

109 A comprehensive field experiment measuring aerosol physical and chemical  
110 properties was conducted from August 2017 to October 2019 at a suburban site in



111 southern Beijing (Fig. 1). Note that this study only employs measurements made  
112 around the 2019 Spring Festival from 16 January to 17 February. This site (39.81°N,  
113 116.48°E) is the test center for meteorological instruments constructed by the China  
114 Meteorological Administration (CMA). It is surrounded by Beijing's 5th Ring Road,  
115 industrial parks, and residential communities (Fig. S1). Aerosol chemical and physical  
116 properties in this area are thus mainly anthropogenic, varying considerably around the  
117 time of the festival in response to the full cycle of industrial activities as the majority  
118 of people stopped and resumed working. This provides an opportunity to investigate  
119 the impact of reduced anthropogenic emissions on surface O<sub>3</sub> and aerosol formation  
120 processes in winter.  
121



122  
123 **Figure 2.** Map showing the Beijing-Tianjin-Hebei region in China and the location of

124 the experiment site. The colored background shows the terrain height (unit: m above  
125 sea level).

126

127 Table 1 lists the instruments used in this campaign. A scanning mobility particle  
128 sizer (SMPS) and an aerodynamic particle sizer (APS) measured the aerosol particle  
129 number size distribution (PNSD) from 10 nm to 20  $\mu\text{m}$ . The SMPS consists of a  
130 differential mobility analyzer (model 3081, TSI Inc.) and a condensation particle  
131 counter (model 3772, TSI Inc.). The aerodynamic diameter measured by the APS can  
132 be converted to the Stokes diameter through division by the square root of the aerosol  
133 density. The aerosol density in this study was calculated following the method of Zhao  
134 et al. (2017), using measured aerosol chemical composition information. An aerosol  
135 chemical speciation monitor (ACSM) equipped with a  $\text{PM}_{2.5}$  lens system, a capture  
136 vaporizer, and a quadrupole mass spectrometer was used to measure mass  
137 concentrations of non-refractory aerosol chemical species in  $\text{PM}_{2.5}$ , including organics  
138 (Org), nitrate ( $\text{NO}_3^-$ ), sulfate ( $\text{SO}_4^{2-}$ ), ammonium ( $\text{NH}_4^+$ ), and chlorine (Chl) (Peck et al.,  
139 2016; Xu et al., 2017; Y. Zhang et al., 2017). A seven-wavelength aethalometer (model  
140 AE-33, Magee Scientific Corp.) with a  $\text{PM}_{2.5}$  cyclone in the sample inlet was used to  
141 retrieve the mass concentration of BC.

142 In addition to the above aerosol measurements, meteorological parameters were  
143 observed by the CMA at the experiment site. The Chinese Ministry of Ecology and  
144 Environment network and Beijing Municipal Environmental Monitoring Center  
145 (<http://106.37.208.233:20035/> and <http://www.bjmemc.com.cn/>) provided  $\text{PM}_{2.5}$  and  
146 trace gas (sulfur dioxide ( $\text{SO}_2$ ), nitrogen dioxide ( $\text{NO}_2$ ), carbon monoxide (CO), and

147 O<sub>3</sub>) measurements made in different locations of the BTH region. Yizhuang in Beijing  
 148 is the nearest station to the experiment site (about 3.0 km to the southeast, Fig. S1). The  
 149 total mass concentrations of measured non-refractory aerosol chemical species and BC  
 150 mass concentrations in PM<sub>2.5</sub> show good consistency with the PM<sub>2.5</sub> mass  
 151 concentrations obtained from the Yizhuang station (Fig. S2).

152

153 **Table 1.** Aerosol instruments used in this campaign and their observed parameters and  
 154 manufacturer information.

Instrument	Measured Parameters	Manufacturer	Model	Time Resolution
SMPS	Particle number size distribution (10–550 nm)	TSI	3938	5 min
APS	Particle number size distribution (0.5–20 μm)	TSI	3321	5 min
ACSM	Mass concentrations of non-refractory aerosol chemical species in PM <sub>2.5</sub>	Aerodyne	Q-ACSM	15 min
Aethalometer	Mass concentration of black carbon	Magee	AE-33	5 min

155

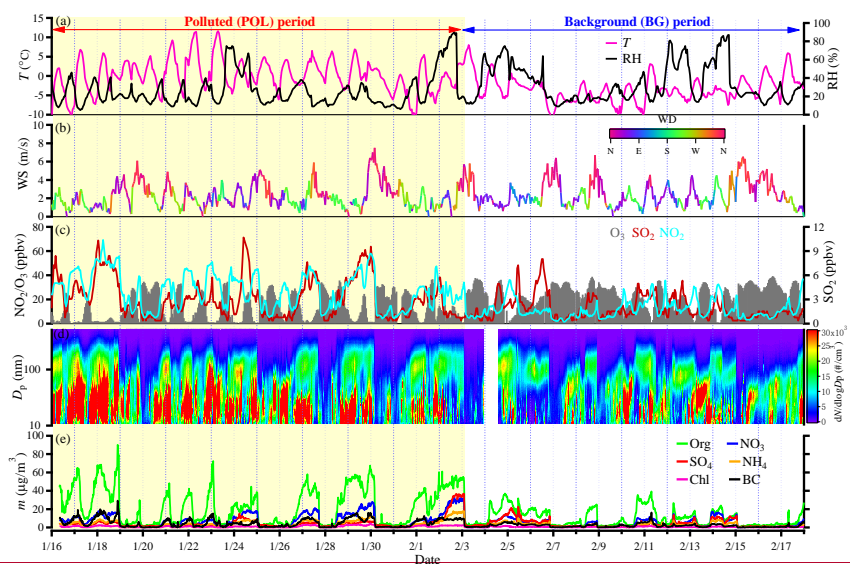
### 156 **3. Results and Discussion**

#### 157 **3.1. Basic meteorological and environmental characteristics**

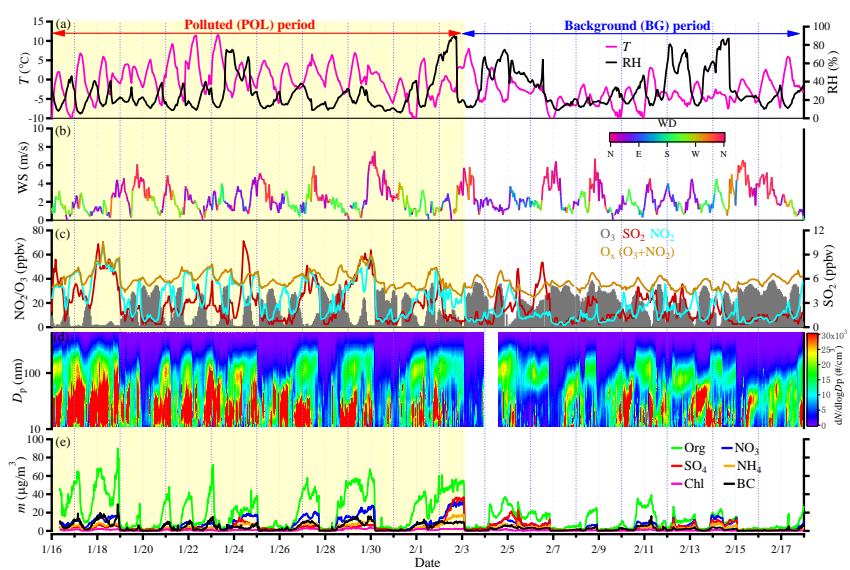
158 While the official Spring Festival holiday was from 4 February to 10 February  
 159 2019, many people left before 3 February and came back after the Lantern Festival (19  
 160 February). In this study, we regarded the days from 16 January to 2 February as the  
 161 polluted (POL) period with high anthropogenic emissions, more representative of  
 162 ordinary conditions, and the days from 3 February to 17 February as the background  
 163 (BG) period with low anthropogenic emissions. Figure 2 shows the time series of  
 164 meteorological parameters, trace gas volume mixing ratios, and aerosol properties

165 during the two periods.

166



167



168

169 **Figure 3.** Time series of (a) ambient temperature ( $T$ ) and relative humidity (RH), (b)

170 wind direction (WD) and speed (WS), (c) volume mixing ratios of trace gases [ $O_3$ ,  $SO_2$ ,

171 ~~and~~ NO<sub>2</sub> ~~and~~ O<sub>x</sub> (O<sub>3</sub>+NO<sub>2</sub>), (d) the aerosol particle number size distribution measured  
172 by the SMPS, and (e) mass concentrations of aerosol chemical species in PM<sub>2.5</sub>  
173 measured by the ACSM and the AE-33. The trace gas information was from the  
174 Yizhuang station, and the others were observed at the experiment site in Beijing (16  
175 January to 17 February 2019).

176

177 Ambient temperature (*T*) and relative humidity (RH) have clear diurnal cycles (Fig.  
178 2a). The average *T* and RH during the BG period were slightly lower ( $-3.3\pm 3.4$  versus  
179  $0.2\pm 4.2^{\circ}\text{C}$ ) and higher ( $33.2\pm 20.1$  versus  $25.8\pm 17.6$  %) than those during the POL  
180 period, respectively. This was caused by several short-term light snowfall events that  
181 occurred on 6, 12, and 14 February during the BG period. Figures 2b and S3 display  
182 similar wind patterns during the POL and BG periods, i.e., wind patterns that changed  
183 periodically. The prevailing, strong northerly winds during the two periods were  
184 beneficial to dispersing pollutants in Beijing (Sun et al., 2016b; Y. Wang et al., 2017),  
185 and thus no heavy haze episodes occurred during these periods. Overall, the  
186 meteorological parameters were similar during the POL and BG periods.

187 Figure 2c ~~illustrates~~~~depicts~~ that the volume mixing ratios of SO<sub>2</sub> and NO<sub>2</sub> ([SO<sub>2</sub>]  
188 and [NSO<sub>2</sub>]) during the BG period were lower than those during the POL period,  
189 suggesting less gaseous pollutants from anthropogenic emissions during the BG period.  
190 In addition, [O<sub>3</sub>] remained at a high level for several days during the BG period but not  
191 during the POL period. The average [O<sub>3</sub>] increased by 77.4 % during the BG period  
192 compared with the POL period ( $46.2\pm 18.9$  versus  $26.1\pm 22.2$  ppbv). The percent change

193 in [O<sub>3</sub>] due to the “holiday effect” during this field campaign is much higher than that  
194 reported in other regions of China (K. Huang et al., 2012; C. Wang et al., 2017; S. Wang  
195 et al., 2019). Figure 2c also shows a weak variation in O<sub>x</sub> (O<sub>3</sub> + NO<sub>2</sub>) from the POL  
196 period to the BG period, indicating that strong O<sub>3</sub>-titration appeared during the Spring  
197 Festival 2019.

198 Many bursts of fine particles (Fig. 2d) occurring mainly during rush hours or at  
199 night were observed during the POL period. This is likely related to the substantial  
200 increases in gasoline or diesel vehicles on two nearby roads at these times. Zhu et al.  
201 (2017) found that efficient nucleation and partitioning of gaseous species from on-road  
202 vehicles can promote new particle formation in the wintertime. However, this  
203 phenomenon occurred much less frequently during the BG period, likely because of the  
204 massive reduction in on-road vehicles. The few short-term bursts of fine particles  
205 during the BG period occurred during the daytime, presumably because of enhanced  
206 nucleation by photochemical processes.

207 The aerosol chemical species in PM<sub>2.5</sub> also differed during the POL and BG periods  
208 (Fig. 2e). During the POL period, the mass concentrations of aerosol chemical species  
209 readily accumulated, especially the organics (*m<sub>org</sub>*) with rapid increases at night. The  
210 mass concentration of BC (*m<sub>BC</sub>*) also clearly increased, likely associated with an  
211 increase in heavy-duty diesel vehicles and a decrease in the nocturnal planetary  
212 boundary layer at night (Y. Wang et al., 2017; Zhao et al., 2017; Z. Li et al., 2017).  
213 However, the increases in *m<sub>org</sub>* and *m<sub>BC</sub>* at night during the BG period were not as strong  
214 as those during the POL period. The mass concentration of nitrate (*m<sub>NO3</sub>*) largely

带格式的: 字体: (默认) Times New Roman, 小四, 字体颜色: 自动设置

带格式的: 字体: (默认) Times New Roman, 小四, 字体颜色: 自动设置

带格式的: 下标

带格式的: 下标

带格式的: 字体: (默认) Times New Roman, 小四, 字体颜色: 自动设置

带格式的: 字体: (默认) Times New Roman, 小四, 字体颜色: 自动设置

带格式的: 字体: (默认) Times New Roman, 小四, 字体颜色: 自动设置

带格式的: 字体: (默认) Times New Roman, 小四, 字体颜色: 自动设置

带格式的: 字体: (默认) Times New Roman, 小四, 字体颜色: 自动设置

带格式的: 非突出显示

215 decreased during the BG period, while there was a weak variation in the mass  
216 concentration of sulfate ( $m_{\text{SO}_4}$ ).

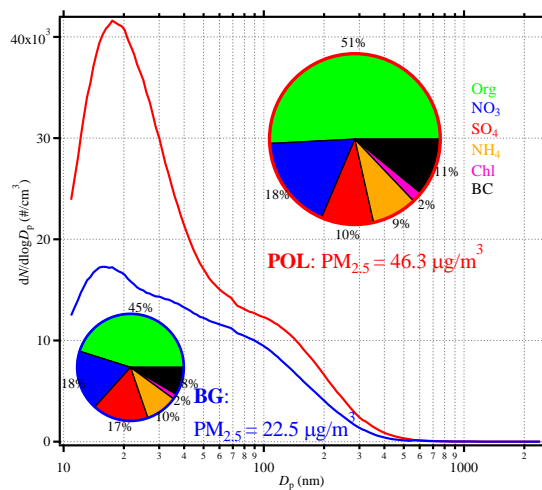
217 In summary, distinct differences existed in all observed trace gases and aerosol  
218 chemical and physical parameters during the POL and BG periods. However, the  
219 meteorological parameters (wind direction and speed, ambient temperature, and RH)  
220 and weather regimes were similar during these two periods. This helps to single out the  
221 impact of reduced anthropogenic emissions on trace gases and aerosol formation  
222 processes.

223

### 224 **3.2. Impact of reduced anthropogenic emissions on aerosol formation processes**

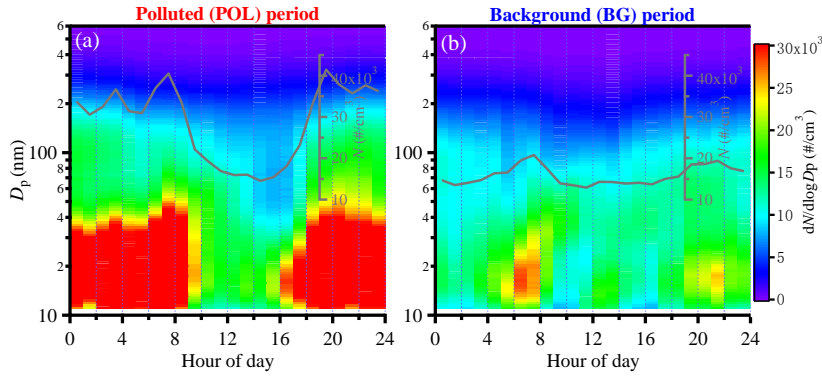
225 The average  $\text{PM}_{2.5}$  mass concentrations were 46.3 and 22.5  $\mu\text{g}/\text{m}^3$  during the POL  
226 and BG periods, respectively. Figure 3 illustrates the average PNSD and aerosol  
227 chemical species in  $\text{PM}_{2.5}$  during the two periods. The particle number concentrations  
228 at all sizes were much higher during the POL period than during the BG period,  
229 especially for ultrafine particles (with diameters, or  $D_p$ , < 100 nm). The diurnal  
230 variation in PNSD during the POL period shown in Fig. 4a suggests that aerosol  
231 particles with  $D_p < 50$  nm burst during rush hours and in the nighttime. The total particle  
232 number concentration ( $N$ ) remained greater than 30,000  $\text{cm}^{-3}$  at these times. However,  
233 during the BG period, the number concentration of ultrafine particles only increased  
234 weakly during rush hours or nucleation times.  $N$  was always less than 20,000  $\text{cm}^{-3}$  on  
235 all days during the BG period (Fig. 4b), probably linked with the reduction in on-road  
236 vehicles during the holiday. As shown in Table 2, the ratio of BG to POL 10–50 nm

237 particle number concentrations ( $N_{10-50 \text{ nm}}$ ) (0.47) is much smaller than the ratios for  
 238 larger particles (0.78 for  $N_{50-100 \text{ nm}}$  and 0.67 for  $N_{>100 \text{ nm}}$ ). These all demonstrate the  
 239 strong impact of reduced anthropogenic emissions on aerosol number concentrations,  
 240 especially for nucleation-mode and small Aitken-mode particles.  
 241



242  
 243 **Figure 4.** Average aerosol particle number size distributions (red and blue curves) and  
 244 mass fractions of aerosol chemical species in PM<sub>2.5</sub> (pie charts with red and blue  
 245 outlines) during the POL (in red) and BG (in blue) periods.  
 246





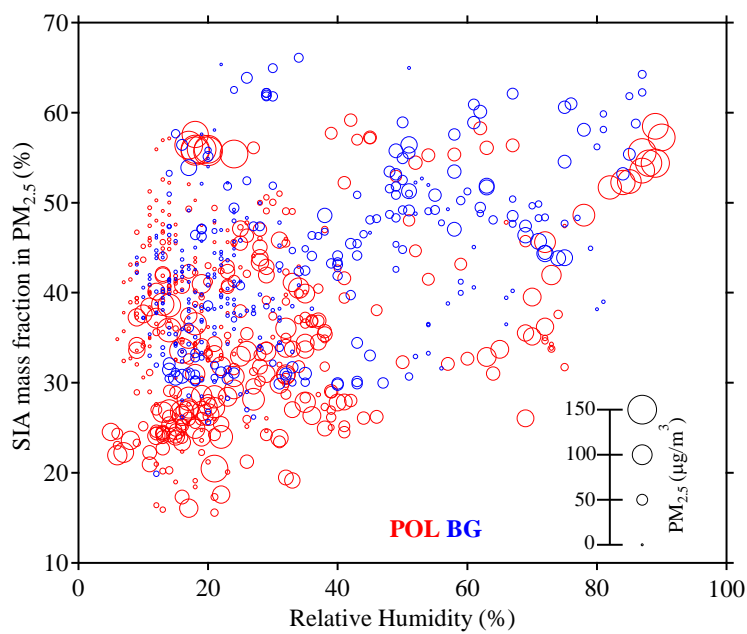
247  
248 **Figure 5.** Diurnal variations in aerosol particle number size distribution (colored  
249 background) and total aerosol number concentration ( $N$ , shown as grey curves) during  
250 the (a) POL and (b) BG periods.

251  
252 **Table 2.** Summary of the average aerosol number concentration ( $N$ ) in different size  
253 ranges, volume mixing ratios of trace gases, mass concentrations of  $PM_{2.5}$  and different  
254 aerosol chemical species, sulfur oxidation ratios (SOR), and nitrogen oxidation ratios  
255 (NOR) during the POL and BG periods and their ratios.

	$N_{10-50\text{ nm}}$ ( $\text{cm}^{-3}$ )	$N_{50-100\text{ nm}}$ ( $\text{cm}^{-3}$ )	$N_{>100\text{ nm}}$ ( $\text{cm}^{-3}$ )	$SO_2$ (ppbv)	$NO_2$ (ppbv)	$O_3$ (ppbv)	$PM_{2.5}$ ( $\mu\text{g}/\text{m}^3$ )
POL	$20,861 \pm 19,935$	$3,946 \pm 2,544$	$3,888 \pm 2,757$	$8.31 \pm 6.35$	$51.96 \pm 27.35$	$26.06 \pm 22.24$	$46.32 \pm 39.05$
BG	$9,837 \pm 8,493$	$3,071 \pm 1,478$	$2,600 \pm 2,223$	$4.85 \pm 3.83$	$21.87 \pm 13.99$	$46.23 \pm 18.86$	$22.52 \pm 20.28$
BG/POL	0.47	0.78	0.67	0.58	0.42	1.77	0.49
	$m_{\text{Org}}$ ( $\mu\text{g}/\text{m}^3$ )	$m_{\text{NO}_3}$ ( $\mu\text{g}/\text{m}^3$ )	$m_{\text{SO}_4}$ ( $\mu\text{g}/\text{m}^3$ )	$m_{\text{NH}_4}$ ( $\mu\text{g}/\text{m}^3$ )	$m_{\text{BC}}$ ( $\mu\text{g}/\text{m}^3$ )	SOR	NOR
POL	$23.55 \pm 19.58$	$8.25 \pm 7.91$	$4.59 \pm 6.20$	$3.96 \pm 3.83$	$5.05 \pm 4.51$	$0.27 \pm 0.17$	$0.09 \pm 0.08$
BG	$10.17 \pm 9.13$	$4.09 \pm 4.25$	$3.82 \pm 4.08$	$2.18 \pm 2.14$	$1.91 \pm 1.74$	$0.32 \pm 0.18$	$0.10 \pm 0.08$
BG/POL	0.43	0.50	0.83	0.55	0.38	1.19	1.11

256  
257 Table 2 also indicates that the mass concentrations ( $m$ ) of aerosol chemical species  
258 in  $PM_{2.5}$  were much less during the BG period than during the POL period clearly  
259 decreased more during the BG period than during the POL period. The  $m$  related to

260 primary emissions ( $m_{\text{org}}$  and  $m_{\text{BC}}$ ) decreased by more than 50 %, but the  $m$  of secondary  
261 inorganic aerosols (SIA, including nitrate, sulfate, and ammonium) slightly decreased,  
262 especially ~~for~~ sulfate ( $m_{\text{SO}_4}$  decreased by only 17 %). The pie charts in Fig. 3 show  
263 significant differences in the aerosol chemical species of  $\text{PM}_{2.5}$  during the two periods.  
264 The mass fractions of Org and BC were lower during the BG period (45 % and 8 %,  
265 respectively) than during the POL period (51 % and 11 %, respectively). By contrast,  
266 the mass fraction of SIA was higher during the BG period (45 %) than during the POL  
267 period (37 %). This indicates that the strongly reduced anthropogenic emissions during  
268 the holiday caused sharp decreases in primary aerosols but not secondary aerosols. The  
269 sulfur oxidation ratio (SOR) and nitrogen oxidation ratio (NOR) are usually calculated  
270 to study the transformation of secondary aerosols (Sun et al., 2006; Y. Li et al., 2017).  
271 SOR (NOR) is defined as the ratio of the molar concentration of sulfate (nitrate) to the  
272 total molar concentration of sulfate (nitrate) and  $\text{SO}_2$  ( $\text{NO}_2$ ). Table 2 shows that SOR  
273 and NOR were higher during the BG period than during the POL period, suggesting  
274 that the formation of secondary inorganics was enhanced during the BG period. Figure  
275 5 shows that most large  $\text{PM}_{2.5}$  mass concentrations ( $> 100 \mu\text{g}/\text{m}^3$ ) during the POL period  
276 occurred along with low RH ( $< 40 \%$ ) and low SIA mass fractions, indicating the  
277 important contribution of primary emissions to the accumulation of  $\text{PM}_{2.5}$  in a polluted  
278 environment. However, large  $\text{PM}_{2.5}$  mass concentrations ( $> 50 \mu\text{g}/\text{m}^3$ ) during the BG  
279 period mainly appeared under moderate RH ( $40 < \text{RH} < 80 \%$ ) and high SIA mass  
280 fraction conditions, likely caused by enhanced aqueous-phase chemical reactions  
281 during this period.



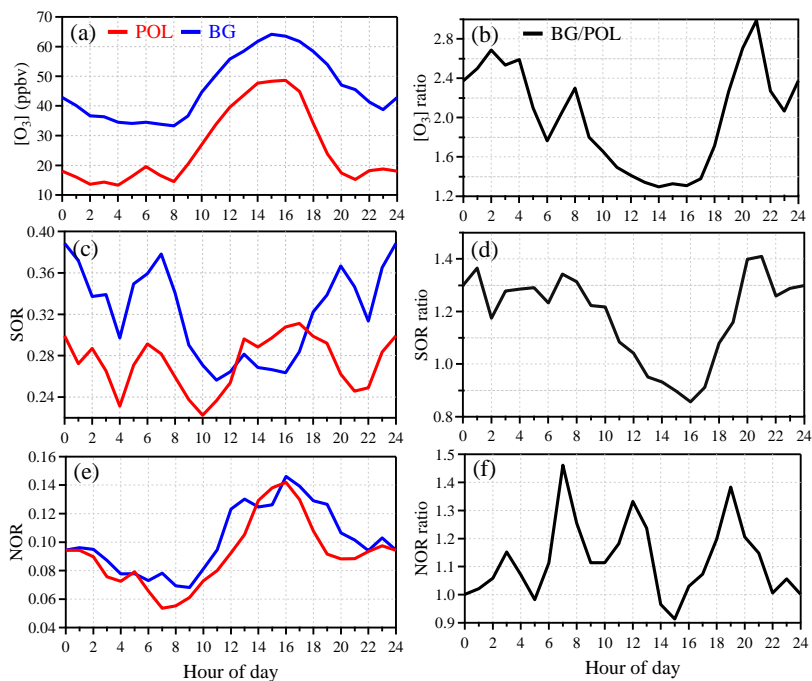
283

284 **Figure 6.** The variation in secondary inorganic aerosols (SIA) mass fraction in  $PM_{2.5}$   
 285 as a function of ambient relative humidity during the POL (in red) and BG (in blue)  
 286 periods. The different circle sizes denote different  $PM_{2.5}$  mass concentrations.

287

288 The diurnal variation in  $[O_3]$  (Fig. 6a) shows more accumulated  $O_3$  during the BG  
 289 period than during the POL period at any time of the day, ~~revealing a stronger~~  
 290 ~~atmospheric oxidation capacity during the BG period.~~ In particular,  $[O_3]$  at night was  
 291 two times higher during the BG period than during the POL period (Fig. 6b). Distinct  
 292 diurnal variations in SOR were found during the two periods (Fig. 6c). The higher SOR  
 293 at night during the BG period (Fig. 6c) indicates the enhanced transformation of  $SO_2$  to  
 294 sulfate, likely related to nocturnal aqueous-phase chemical reactions due to the elevated

295 ambient RH at night (Fig. S4). Figure S54 indicates that SOR increased following an  
296 increase in ALWC when the ambient RH was higher than ~40 % during the BG period.  
297 Moreover, Fig. 6d shows that the diurnal variation in the SOR ratio during the two  
298 periods was similar to that of the [O<sub>3</sub>] ratio. This suggests that sulfate formation during  
299 the holiday was likely enhanced by nocturnal aqueous-phase chemical reactions  
300 between SO<sub>2</sub> and O<sub>3</sub>. This is consistent with the study of Fang et al. (2019), which found  
301 that ambient RH and the O<sub>3</sub> concentration are two prerequisites for rapid sulfate  
302 formation via aqueous-phase oxidation reactions. This result highlights that controlling  
303 O<sub>3</sub> formation under current emission conditions in winter in Beijing is key to further  
304 reducing the formation of sulfate and implies that the high underestimation of sulfate  
305 at night in models (Miao et al., 2020) could be caused by an~~the~~ inaccurate simulation  
306 of [O<sub>3</sub>]. The higher daytime NOR (Fig. 6e) than nighttime NOR during the two periods  
307 illustrates that the formation of nitrate was mainly controlled by photochemical  
308 reactions in winter. Figure 6f shows that the larger NOR difference (the higher NOR  
309 ratio) during rush hours during the two periods likely occurred because a mass of  
310 emitted NO<sub>x</sub> during rush hours could not be transformed to nitrate during the POL  
311 period. Figure 6e and 6f also suggests nitrate formation was somewhat enhanced ~~a little~~  
312 during the holiday likely due to ~~the~~ enhanced daytime photochemical reactions.



313  
 314 **Figure 7.** Diurnal variations in (a and b) O<sub>3</sub> volume mixing ratio and its ratio, (c and  
 315 **d)** sulfur oxidation ratio (SOR) and its ratio, and (e and f) nitrogen oxidation ratio  
 316 (NOR) and its ratio during the BG and POL periods. The ratio of a quantity is that  
 317 quantity during the BG period divided by that quantity during the POL period.

318

319 Overall, the reduced anthropogenic emissions led to a drastic decrease in aerosol  
 320 particle number concentration during the holiday. However, the general enhancement  
 321 of [O<sub>3</sub>] atmospheric oxidation capacity was enhanced during the holiday, thereby could  
 322 promoting the formation of secondary inorganics (especially sulfate).

323  
 324  
 325

带格式的: 下标

326 **3.3. Impact of reduced anthropogenic emissions on regional air pollution**

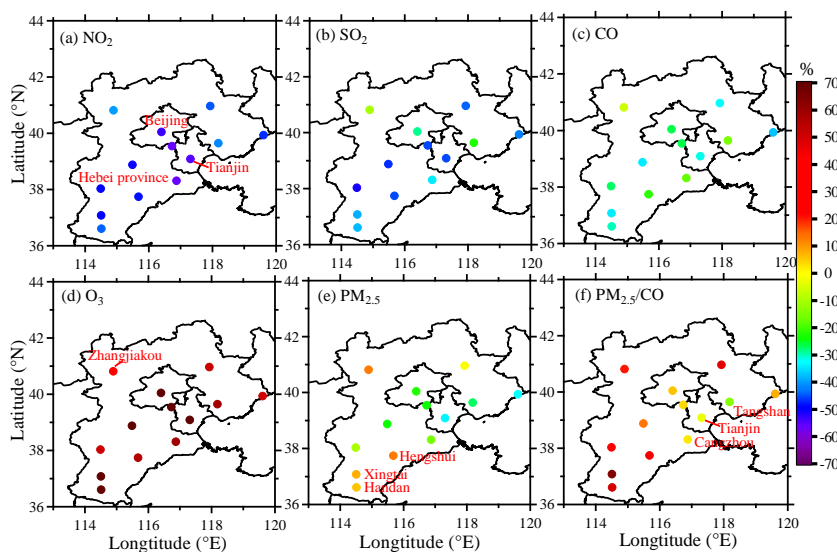
327 Figure 7a-c shows that the volume mixing ratios of emitted trace gases ([SO<sub>2</sub>],  
 328 [NO<sub>2</sub>], and [CO]) decreased in the Beijing-Tianjin-Hebei (BTH) region during the BG  
 329 period. [NO<sub>2</sub>] and [SO<sub>2</sub>] decreased by more than 40 % in all cities and 35 % in heavy-  
 330 industry cities (distributed in the southern and northeastern parts of the BTH region).

331 This indicates a regional reduction in anthropogenic emissions during the holiday.

332 Figure 7d shows that [O<sub>3</sub>] increased in all cities and that the increase was more than  
 333 50 % in all cities except for a high-altitude city (Zhangjiakou) to the northwest,  
 334 implying the regional enhancement of the atmospheric oxidation capacity.

335

带格式的: 图案: 清除



336

337 **Figure 8.** Percent changes in trace gas volume mixing ratios (NO<sub>2</sub>, SO<sub>2</sub>, CO, and O<sub>3</sub>),

338 the PM<sub>2.5</sub> mass concentration, and the PM<sub>2.5</sub>/CO ratio during the BG period relative to

339 the POL period:  $100 \times \left( \frac{[BG] - [POL]}{[POL]} \right)$  in the Beijing-Tianjin-Hebei (BTH) region.

340

341 The PM<sub>2.5</sub> mass concentration decreased at a much lower rate relative to the  
342 decrease in [NO<sub>2</sub>] and [SO<sub>2</sub>] in most cities during the BG period (Fig. 7e), while it  
343 increased slightly at Zhangjiakou and three southern heavy-industry cities (Hengshui,  
344 Xingtai, and Handan). The ratio PM<sub>2.5</sub>/CO is an indicator of aerosol secondary  
345 formation to primary emissions. An increase in PM<sub>2.5</sub>/CO was found during the BG  
346 period at all cities except for three coastal cities (Tangshan, Tianjin, and Cangzhou),  
347 revealing the regional enhancement of secondary aerosol formation during the  
348 holiday. The weak decrease in PM<sub>2.5</sub>/CO at the three coastal cities was likely due to  
349 the influence of mixed sea flows.

350 The regional analysis of air pollution assumes that the findings from Beijing  
351 presented in section 3.2 are applicable to the entire BTH region. Regionally reduced  
352 anthropogenic emissions resulted in sharply decreased gaseous pollutants and  
353 increased O<sub>3</sub>. ~~Higher atmospheric oxidation led to t~~The enhanced formation of  
354 secondary aerosols likely due to enhanced aqueous chemical reactions involving O<sub>3</sub>  
355 ~~could, thus~~ counteracting the decrease in PM<sub>2.5</sub> mass concentration. There are two  
356 possible reasons explaining the high [O<sub>3</sub>] during the holiday: (1) the reduced gaseous  
357 precursors (NO<sub>x</sub> and SO<sub>2</sub>) weakened the consumption of O<sub>3</sub>, and (2) O<sub>3</sub> formation in  
358 the BTH region is likely volatile organic compound (VOC)-controlled under current  
359 emission conditions, therefore the reduction in NO<sub>x</sub> would lead to higher [O<sub>3</sub>]. ~~This~~  
360 All these results demonstrates that it is ~~more~~ important to reduce O<sub>3</sub> formation ~~VOC~~  
361 ~~emissions~~ to further control PM<sub>2.5</sub> in winter in the BTH region.

带格式的: 下标

带格式的: 下标

364

#### 365 **4. Conclusions and Implications**

366 In recent years, the mass concentration of particulate matter with an aerodynamic  
367 diameter of less than 2.5  $\mu\text{m}$  ( $\text{PM}_{2.5}$ ) has shown a general decreasing trend, presumably  
368 due to the series of emission reduction measures taken in China ~~in an attempt~~ing to  
369 improve air quality. However, haze pollution episodes still occur from time to time,  
370 including during some special events when primary emissions reduced drastically, such  
371 as the Chinese New Year holiday and even during the COVID-19 lockdown when  
372 anthropogenic activities diminished ~~dramatically~~drastically (X. Huang et al., 2020). We  
373 conjecture that reductions through primary emissions may be offset by increases in the  
374 formation of secondary aerosols.

375 To test this, we examined the secondary aerosol formation mechanism in a  
376 comprehensive field experiment conducted in Beijing. ~~Comprehensive a~~Aerosol and  
377 meteorological measurements were made for more than two years, but data around the  
378 2019 Chinese Spring Festival from 16 January to 17 February were employed in this  
379 study to single out the impact of emission reductions due to the holiday. The study  
380 period was divided into polluted (POL) and background (BG) periods, with high and  
381 low anthropogenic emissions before and during the festival holiday, respectively.  
382 Investigated were the impacts of reduced anthropogenic emissions on trace gases and  
383  $\text{PM}_{2.5}$  under similar meteorological conditions.

384 The average  $\text{PM}_{2.5}$  mass concentrations were 46.3 and 22.5  $\mu\text{g}/\text{m}^3$  during the POL  
385 and BG periods, respectively, with no heavy haze events occurring. The average aerosol



386 particle number size distribution shows that the reduced anthropogenic emissions  
387 during the holiday led to decreased aerosol number concentrations at all sizes,  
388 especially in the nucleation and Aitken modes (mobility diameters less than 50 nm).  
389 Simultaneously, the reduced anthropogenic emissions resulted in decreases in the  
390 volume mixing ratios of SO<sub>2</sub> and NO<sub>2</sub> and an unexpected increase in the volume mixing  
391 ratio of O<sub>3</sub> [O<sub>3</sub>] during the BG period caused by the appeared O<sub>3</sub>-titration phenomenon.

带格式的: 下标

392 The analysis of the aerosol chemical species in PM<sub>2.5</sub> demonstrates that the large  
393 decreases in organics and black carbon mass concentrations during the BG period were  
394 likely caused by the large decrease in on-road vehicles. Moreover, the mass  
395 concentration of nitrate also decreased while that of sulfate decreased much less during  
396 the BG period. Comparisons of the sulfur oxidation ratio (SOR) and the nitrogen  
397 oxidation ratio (NOR) during the two periods imply that the transformation of gaseous  
398 precursors to secondary inorganics (especially the transformation of SO<sub>2</sub> to sulfate) was  
399 promoted during the BG period, likely due to the enhanced atmospheric-aqueous  
400 chemical reactions involving the dissolved O<sub>3</sub>oxidation capacity. The diurnal variation

带格式的: 下标

401 in the SOR ratio between the BG and POL periods was similar to that of the [O<sub>3</sub>] ratio,  
402 illustrating that sulfate formation was promoted by the enhanced nocturnal aqueous-  
403 phase chemical reactions between SO<sub>2</sub> and O<sub>3</sub> under moderate relative humidity (RH)  
404 conditions (40 % < RH < 80 %). The higher NOR in the daytime during the two periods  
405 points out that the formation of nitrate was mainly controlled by photochemical  
406 reactions and weakly affected by the increase in [O<sub>3</sub>].

407 This study also investigated the impact of reduced anthropogenic emissions on

408 regional air pollution patterns during the holiday. The variation trends of trace gases in  
409 most cities in the Beijing-Tian-Hebei (BTH) region were similar to those in Beijing,  
410 indicating the regional influence of reduced anthropogenic emissions on the volume  
411 mixing ratios of trace gases during the holiday. The weak PM<sub>2.5</sub> variation and the  
412 increased PM<sub>2.5</sub>/CO ratio (an indicator of aerosol secondary formation to primary  
413 emissions) during the BG period both suggest that the enhanced formation of secondary  
414 aerosols offset the regional decrease in PM<sub>2.5</sub> during the holiday.

415 Our findings provide evidence that decreases in anthropogenic emissions can  
416 promote the formation of secondary inorganics due to the enhancement of aqueous  
417 reactions likely caused by the increased [O<sub>3</sub>]. This result implies that haze mitigation  
418 in north China needs a coordinated and balanced strategy for controlling multiple  
419 pollutants, the atmospheric oxidation capacity (manifested by more accumulated O<sub>3</sub>).  
420 ~~In the future, the simultaneous control of PM<sub>2.5</sub> and O<sub>3</sub> will be needed to further reduce~~  
421 ~~air pollution. The O<sub>3</sub> formation in winter in the BTH region is possibly volatile organic~~  
422 ~~compound (VOC) controlled under current emission conditions. Controlling VOC~~  
423 ~~emissions may thus be more important than controlling emissions of nitrogen oxides.~~

424  
425  
426 *Acknowledgement.* This work was funded by the National Key R&D Program of the  
427 Ministry of Science and Technology, China (Grant No. 2017YFC1501702) and the  
428 National Natural Science Foundation of China (NSFC) research project (grant no.  
429 42005067), and the Open Fund of State Key Laboratory of Remote Sensing Science  
430 (grant no. 202015). Startup Foundation for Introducing Talent of NUIST (No.  
431 2019r077).

432

带格式的: 下标

带格式的: 行距: 1.5 倍行距, 孤行控制, 边框: 顶端: (无框线), 底端: (无框线), 左侧: (无框线), 右侧: (无框线), 介于: (无框线), 竖线: (无框线)

带格式的: 字体: (中文) Adobe 繁黑體 Std B, 小四

带格式的: 字体: (中文) Adobe 繁黑體 Std B, 小四

带格式的: 字体: (中文) Adobe 繁黑體 Std B, 小四

433 *Data availability.* Data from the Chinese Ministry of Ecology and Environment  
434 network and Beijing Municipal Environmental Monitoring Center can be downloaded  
435 from the websites given in the main text. The measurement data from the field  
436 experiment used in this study are available from the first author upon request  
437 (yuyingwang@nuist.edu.cn).

438

439 *Author contributions.* ZL and PY designed the field experiment. YW and ZL  
440 conceived the study and led the overall scientific questions. YW, QW, and XJ  
441 processed the measurement data and prepared this paper. MC copyedited the article.

442 Other co-authors participated in the implementation of this experiment and the  
443 discussion of this paper.

444

445 *Competing interests.* The authors declare that they have no conflict of interest.

446

## 447 **References**

448

449 Altaratz, O., Koren, I., Remer, L. A., and Hirsch, E.: Review: Cloud invigoration by aerosols—coupling  
450 between microphysics and dynamics, *Atmos. Res.*, 140, 38–60,  
451 <https://doi.org/10.1016/j.atmosres.2014.01.009>, 2014.

452 An, Z., Huang, R., Zhang, R., Tie, X., Li, G., Cao, J., Zhou, W., Shi, Z., Han, Y., Gu, Z., and Ji, Y.:  
453 Severe haze in northern China: a synergy of anthropogenic emissions and atmospheric processes, *Proc.*  
454 *Natl. Acad. Sci. U.S.A.*, 116, 8657, <https://doi.org/10.1073/pnas.1900125116>, 2019.

455 Chan, C. K., and Yao, X.: Air pollution in megacities in China, *Atmos. Environ.*, 42, 1–42,  
456 <https://doi.org/10.1016/j.atmosenv.2007.09.003>, 2008.

457 Chow, J. C., Watson, J. G., Mauderly, J. L., Costa, D. L., Wyzga, R. E., Vedal, S., Hidy, G. M., Altshuler,  
458 S. L., Marrack, D., Heuss, J. M., Wolff, G. T., Arden Pope III, C., and Dockery, D. W.: Health effects  
459 of fine particulate air pollution: lines that connect, *J. Air Waste Manage.*, 56, 1368–1380,  
460 <https://doi.org/10.1080/10473289.2006.10464545>, 2006.

461 Fang, Y., Ye, C., Wang, J., Wu, Y., Hu, M., Lin, W., Xu, F., and Zhu, T.: Relative humidity and O<sub>3</sub>  
462 concentration as two prerequisites for sulfate formation, *Atmos. Chem. Phys.*, 19, 12,295–12,307,  
463 <https://doi.org/10.5194/acp-19-12295-2019>, 2019.

464 Gao, J., Woodward, A., Vardoulakis, S., Kovats, S., Wilkinson, P., Li, L., Xu, L., Li, J., Yang, J., Li, J.,  
465 Cao, L., Liu, X., Wu, H., and Liu, Q.: Haze, public health and mitigation measures in China: a review  
466 of the current evidence for further policy response, *Sci. Total Environ.*, 578, 148–157,  
467 <https://doi.org/10.1016/j.scitotenv.2016.10.231>, 2017.

468 Guo, S., Hu, M., Guo, Q., Zhang, X., Schauer, J. J., and Zhang, R.: Quantitative evaluation of emission  
469 controls on primary and secondary organic aerosol sources during Beijing 2008 Olympics, *Atmos.*  
470 *Chem. Phys.*, 13, 8303–8314, <https://doi.org/10.5194/acp-13-8303-2013>, 2013.

471 Guo, S., Hu, M., Zamora, M. L., Peng, J., Shang, D., Zheng, J., Du, Z., Wu, Z., Shao, M., Zeng, L.,  
472 Molina, M. J., and Zhang, R.: Elucidating severe urban haze formation in China, *Proc. Natl. Acad.*  
473 *Sci. U.S.A.*, 111, 17373, <https://doi.org/10.1073/pnas.1419604111>, 2014.

474 Han, L., Zhou, W., Li, W., and Li, L.: Impact of urbanization level on urban air quality: a case of fine  
475 particles (PM<sub>2.5</sub>) in Chinese cities, *Environ. Pollut.*, 194, 163–170,  
476 <https://doi.org/10.1016/j.envpol.2014.07.022>, 2014.

477 Huang, K., Zhuang, G., Lin, Y., Wang, Q., Fu, J. S., Zhang, R., Li, J., Deng, C., and Fu, Q.: Impact of  
478 anthropogenic emission on air quality over a megacity revealed from an intensive atmospheric  
479 campaign during the Chinese Spring Festival, *Atmos. Chem. Phys.*, 12, 11,631–11,645,  
480 <https://doi.org/10.5194/acp-12-11631-2012>, 2012.

481 Huang, X., Ding, A., Gao, J., Zheng, B., Zhou, D., Qi, X., Tang, R., Wang, J., Ren, C., Nie, W., Chi, X.,  
482 Wang, J., Xu, Z., Chen, L., Li, Y., Che, F., Pang, N., Wang, H., Tong, D., Qin, W., Cheng, W., Liu,  
483 W., Fu, Q., Liu, B., Chai, F., Davis, S. J., Zhang, Q. and He, K.: Enhanced secondary pollution offset  
484 reduction of primary emissions during COVID-19 lockdown in China, [National Science Review](https://doi.org/10.1093/nsr/nwaa13740.31223/af.104wvzy),  
485 <https://doi.org/10.1093/nsr/nwaa13740.31223/af.104wvzy>, 2020.

486 Jin, X., Wang, Y., Li, Z., Zhang, F., Xu, W., Sun, Y., Fan, X., Chen, G., Wu, H., Ren, J., Wang, Q., and  
487 Cribb, M.: Significant contribution of organics to aerosol liquid water content in winter in Beijing,  
488 China, *Atmos. Chem. Phys.*, 20, 901–914, <https://doi.org/10.5194/acp-20-901-2020>, 2020.

489 Li, H., Cheng, J., Zhang, Q., Zheng, B., Zhang, Y., Zheng, G., and He, K.: Rapid transition in winter  
490 aerosol composition in Beijing from 2014 to 2017: response to clean air actions, *Atmos. Chem. Phys.*,  
491 19, 11,485–11,499, <https://doi.org/10.5194/acp-19-11485-2019>, 2019a.

492 Li, H., Wang, D., Cui, L., Gao, Y., Huo, J., Wang, X., Zhang, Z., Tan, Y., Huang, Y., Cao, J., Chow, J.  
493 C., Lee, S., and Fu, Q.: Characteristics of atmospheric PM<sub>2.5</sub> composition during the implementation  
494 of stringent pollution control measures in Shanghai for the 2016 G20 summit, *Sci. Total Environ.*, 648,  
495 1121–1129, <https://doi.org/10.1016/j.scitotenv.2018.08.219>, 2019b.

496 Li, K., Jacob, D. J., Liao, H., Shen, L., Zhang, Q., and Bates, K. H.: Anthropogenic drivers of 2013–  
497 2017 trends in summer surface ozone in China, *P. Natl. Acad. Sci. U.S.A.*, 116, 422–427,  
498 <https://doi.org/10.1073/pnas.1812168116>, 2019.

499 Li, K., Jacob, D. J., Shen, L., Lu, X., De Smedt, I., and Liao, H.: 2013–2019 increases of surface ozone  
500 pollution in China: anthropogenic and meteorological influences, *Atmos. Chem. Phys. Discuss.*, 2020,  
501 1–18, <https://doi.org/10.5194/acp-2020-298>, 2020.

502 Li, Y. J., Sun, Y., Zhang, Q., Li, X., Li, M., Zhou, Z., and Chan, C. K.: Real-time chemical  
503 characterization of atmospheric particulate matter in China: a review, *Atmos. Environ.*, 158, 270–304,  
504 <https://doi.org/10.1016/j.atmosenv.2017.02.027>, 2017.

505 Li, Z., Lau, W. K. M., Ramanathan, V., Wu, G., Ding, Y., Manoj, M. G., Liu, J., Qian, Y., Li, J., Zhou,  
506 T., Fan, J., Rosenfeld, D., Ming, Y., Wang, Y., Huang, J., Wang, B., Xu, X., Lee, S. S., Cribb, M.,  
507 Zhang, F., Yang, X., Zhao, C., Takemura, T., Wang, K., Xia, X., Yin, Y., Zhang, H., Guo, J., Zhai, P.

带格式的: 字体: (默认) Times New Roman, (中文) + 中文  
正文 (等线), 10 磅, 字体颜色: 自动设置, 英语(美国)

508 M., Sugimoto, N., Babu, S. S., and Brasseur, G. P.: Aerosol and monsoon climate interactions over  
509 Asia, *Rev. Geophys.*, 54, 866–929, <https://doi.org/10.1002/2015RG000500>, 2016.

510 Li, Z., Guo, J., Ding, A., Liao, H., Liu, J., Sun, Y., Wang, T., Xue, H., Zhang, H., and Zhu, B.: Aerosol  
511 and boundary-layer interactions and impact on air quality, *Natl. Sci. Rev.*, 4, 810–833,  
512 <https://doi.org/10.1093/nsr/nwx117>, 2017.

513 Li, Z., Wang, Y., Guo, J., Zhao, C., Cribb, M. C., Dong, X., Fan, J., Gong, D., Huang, J., Jiang, M., Jiang,  
514 Y., Lee, S. S., Li, H., Li, J., Liu, J., Qian, Y., Rosenfeld, D., Shan, S., Sun, Y., Wang, H., Xin, J., Yan,  
515 X., Yang, X., Yang, X., Zhang, F., and Zheng, Y.: East Asian Study of Tropospheric Aerosols and  
516 their Impact on Regional Clouds, Precipitation, and Climate (EAST-AIRCPC), *J. Geophys. Res.*  
517 *Atmos.*, 124, 13,026–13,054, <https://doi.org/10.1029/2019JD030758>, 2019.

518 Matus, K., Nam, K., Selin, N. E., Lamsal, L. N., Reilly, J. M., and Paltsev, S.: Health damages from air  
519 pollution in China, *Global Environ. Change*, 22, 55–66,  
520 <https://doi.org/10.1016/j.gloenvcha.2011.08.006>, 2012.

521 Miao, R., Chen, Q., Zheng, Y., Cheng, X., Sun, Y., Palmer, P. I., Shrivastava, M., Guo, J., Zhang, Q.,  
522 Liu, Y., Tan, Z., Ma, X., Chen, S., Zeng, L., Lu, K., and Zhang, Y.: Model bias in simulating major  
523 chemical components of PM<sub>2.5</sub> in China, *Atmos. Chem. Phys. Discuss.*, 2020, 1–33,  
524 <https://doi.org/10.5194/acp-2020-76>, 2020.

525 Peck, J., Gonzalez, L. A., Williams, L. R., Xu, W., Croteau, P. L., Timko, M. T., Jayne, J. T., Worsnop,  
526 D. R., Miake-Lye, R. C., and Smith, K. A.: Development of an aerosol mass spectrometer lens system  
527 for PM<sub>2.5</sub>, *Aerosol Sci. Tech.*, 50, 781–789, <https://doi.org/10.1080/02786826.2016.1190444>, 2016.

528 Seinfeld, J. H., and Pandis, S. N.: *Atmospheric chemistry and physics: from air pollution to climate  
529 change*, edited, John Wiley & Sons, 2016.

530 Sun, Y., Zhuang, G., Tang, A., Wang, Y., and An, Z.: Chemical characteristics of PM<sub>2.5</sub> and PM<sub>10</sub> in  
531 haze-fog episodes in Beijing, *Environ. Sci. Technol.*, 40, 3148–3155,  
532 <https://doi.org/10.1021/es051533g>, 2006.

533 Sun, Y., Chen, C., Zhang, Y., Xu, W., Zhou, L., Cheng, X., Zheng, H., Ji, D., Li, J., Tang, X., Fu, P., and  
534 Wang, Z.: Rapid formation and evolution of an extreme haze episode in Northern China during winter  
535 2015, *Sci. Rep.-UK*, 6, <https://doi.org/10.1038/srep27151>, 2016a.

536 Sun, Y., Wang, Z., Wild, O., Xu, W., Chen, C., Fu, P., Du, W., Zhou, L., Zhang, Q., Han, T., Wang, Q.,  
537 Pan, X., Zheng, H., Li, J., Guo, X., Liu, J., and Worsnop, D. R.: “APEC Blue” : secondary aerosol  
538 reductions from emission controls in Beijing, *Sci. Rep.-UK*, 6, 20668,  
539 <https://doi.org/10.1038/srep20668>, 2016b.

540 Tan, P., Chou, C., Liang, J., Chou, C. C. K., and Shiu, C.: Air pollution “holiday effect” resulting  
541 from the Chinese New Year, *Atmos. Environ.*, 43, 2114–2124,  
542 <https://doi.org/10.1016/j.atmosenv.2009.01.037>, 2009.

543 Vu, D., Gao, S., Berte, T., Kacarab, M., Yao, Q., Vafai, K., and Asa-Awuku, A.: External and internal  
544 cloud condensation nuclei (CCN) mixtures: controlled laboratory studies of varying mixing states,  
545 *Atmos. Meas. Tech.*, 12, 4277–4289, <https://doi.org/10.5194/amt-12-4277-2019>, 2019.

546 Wang, C., Huang, X. F., Zhu, Q., Cao, L. M., Zhang, B., and He, L. Y.: Differentiating local and regional  
547 sources of Chinese urban air pollution based on the effect of the Spring Festival, *Atmos. Chem. Phys.*,  
548 17, 9103–9114, <https://doi.org/10.5194/acp-17-9103-2017>, 2017.

549 Wang, S., Yu, R., Shen, H., Wang, S., Hu, Q., Cui, J., Yan, Y., Huang, H., and Hu, G.: Chemical  
550 characteristics, sources, and formation mechanisms of PM<sub>2.5</sub> before and during the Spring Festival in  
551 a coastal city in Southeast China, *Environ. Pollut.*, 251, 442–452,

552 <https://doi.org/10.1016/j.envpol.2019.04.050>, 2019.

553 Wang, T., Nie, W., Gao, J., Xue, L. K., Gao, X. M., Wang, X. F., Qiu, J., Poon, C. N., Meinardi, S.,  
554 Blake, D., Wang, S. L., Ding, A. J., Chai, F. H., Zhang, Q. Z., and Wang, W. X.: Air quality during  
555 the 2008 Beijing Olympics: secondary pollutants and regional impact, *Atmos. Chem. Phys.*, 10, 7603–  
556 7615, <https://doi.org/10.5194/acp-10-7603-2010>, 2010.

557 Wang, T., Xue, L., Brimblecombe, P., Lam, Y. F., Li, L., and Zhang, L.: Ozone pollution in China: a  
558 review of concentrations, meteorological influences, chemical precursors, and effects, *Sci. Total*  
559 *Environ.*, 575, 1582–1596, <https://doi.org/10.1016/j.scitotenv.2016.10.081>, 2017.

560 Wang, Y., Zhang, F., Li, Z., Tan, H., Xu, H., Ren, J., Zhao, J., Du, W., and Sun, Y.: Enhanced  
561 hydrophobicity and volatility of submicron aerosols under severe emission control conditions in  
562 Beijing, *Atmos. Chem. Phys.*, 17, 5239–5251, <https://doi.org/10.5194/acp-17-5239-2017>, 2017.

563 Wang, Y., Li, Z., Zhang, Y., Du, W., Zhang, F., Tan, H., Xu, H., Fan, T., Jin, X., Fan, X., Dong, Z.,  
564 Wang, Q., and Sun, Y.: Characterization of aerosol hygroscopicity, mixing state, and CCN activity at  
565 a suburban site in the central North China Plain, *Atmos. Chem. Phys.*, 18, 11,739–11,752,  
566 <https://doi.org/10.5194/acp-18-11739-2018>, 2018.

567 Wang, Y., Chen, J., Wang, Q., Qin, Q., Ye, J., Han, Y., Li, L., Zhen, W., Zhi, Q., Zhang, Y., and Cao,  
568 J.: Increased secondary aerosol contribution and possible processing on polluted winter days in China,  
569 *Environ. Int.*, 127, 78–84, <https://doi.org/10.1016/j.envint.2019.03.021>, 2019a.

570 Wang, Y., Li, Z., Zhang, R., Jin, X., Xu, W., Fan, X., Wu, H., Zhang, F., Sun, Y., Wang, Q., Cribb, M.,  
571 and Hu, D.: Distinct ultrafine- and accumulation-mode particle properties in clean and polluted urban  
572 environments, *Geophys. Res. Lett.*, 46, 10,918–10,925, [10.1029/2019GL084047](https://doi.org/10.1029/2019GL084047), 2019b.

573 [Xie, Y., Wang, G., Wang, X., Chen, J., Chen, Y., Tang, G., Wang, L., Ge, S., Xue, G., Wang, Y., and](#)  
574 [Gao, J.: Nitrate-dominated PM<sub>2.5</sub> and elevation of particle pH observed in urban Beijing during the](#)  
575 [winter of 2017, \*Atmos. Chem. Phys.\*, 20, 5019-5033, \[10.5194/acp-20-5019-2020\]\(https://doi.org/10.5194/acp-20-5019-2020\), 2020.](#)

576 Xu, W., Croteau, P., Williams, L., Canagaratna, M., Onasch, T., Cross, E., Zhang, X., Robinson, W.,  
577 Worsnop, D., and Jayne, J.: Laboratory characterization of an aerosol chemical speciation monitor  
578 with PM<sub>2.5</sub> measurement capability, *Aerosol Sci. Tech.*, 51, 69–83,  
579 <https://doi.org/10.1080/02786826.2016.1241859>, 2017.

580 Xu, W., Sun, Y., Wang, Q., Zhao, J., Wang, J., Ge, X., Xie, C., Zhou, W., Du, W., Li, J., Fu, P., Wang,  
581 Z., Worsnop, D. R., and Coe, H.: Changes in aerosol chemistry from 2014 to 2016 in winter in Beijing:  
582 insights from high-resolution aerosol mass spectrometry, *J. Geophys. Res. Atmos.*, 124, 1132–1147,  
583 <https://doi.org/10.1029/2018JD029245>, 2019.

584 Zhai, S., Jacob, D. J., Wang, X., Shen, L., Li, K., Zhang, Y., Gui, K., Zhao, T., and Liao, H.: Fine  
585 particulate matter (PM<sub>2.5</sub>) trends in China, 2013–2018: separating contributions from anthropogenic  
586 emissions and meteorology, *Atmos. Chem. Phys.*, 19, 11,031–11,041, <https://doi.org/10.5194/acp-19-11031-2019>, 2019.

588 Zhang, F., Wang, Y., Peng, J., Chen, L., Sun, Y., Duan, L., Ge, X., Li, Y., Zhao, J., Liu, C., Zhang, X.,  
589 Zhang, G., Pan, Y., Wang, Y., Zhang, A. L., Ji, Y., Wang, G., Hu, M., Molina, M. J., and Zhang, R.:  
590 An unexpected catalyst dominates formation and radiative forcing of regional haze, *Proc. Natl. Acad.*  
591 *Sci. U.S.A.*, 117, 3960, <https://doi.org/10.1073/pnas.1919343117>, 2020.

592 Zhang, Q., Zheng, Y., Tong, D., Shao, M., Wang, S., Zhang, Y., Xu, X., Wang, J., He, H., Liu, W., Ding,  
593 Y., Lei, Y., Li, J., Wang, Z., Zhang, X., Wang, Y., Cheng, J., Liu, Y., Shi, Q., Yan, L., Geng, G.,  
594 Hong, C., Li, M., Liu, F., Zheng, B., Cao, J., Ding, A., Gao, J., Fu, Q., Huo, J., Liu, B., Liu, Z., Yang,  
595 F., He, K., and Hao, J.: Drivers of improved PM<sub>2.5</sub> air quality in China from 2013 to 2017, *P. Natl.*

带格式的: 字体: (默认) Times New Roman, (中文) + 中文  
正文 (等线), 10 磅, 字体颜色: 自动设置, 英语(美国)

596 Acad. Sci. U.S.A., 116, 24,463–24,469, <https://doi.org/10.1073/pnas.1907956116>, 2019.

597 Zhang, R., Wang, G., Guo, S., Zamora, M. L., Ying, Q., Lin, Y., Wang, W., Hu, M., and Wang, Y.:  
598 Formation of urban fine particulate matter, *Chem. Rev.*, 115, 3803–3855,  
599 <https://doi.org/10.1021/acs.chemrev.5b00067>, 2015.

600 Zhang, Y., Sun, Y., Du, W., Wang, Q., Chen, C., Han, T., Lin, J., Zhao, J., Xu, W., Gao, J., Li, J., Fu, P.,  
601 Wang, Z., and Han, Y.: Response of aerosol composition to different emission scenarios in Beijing,  
602 China, *Sci. Total Environ.*, 571, 902–908, <https://doi.org/10.1016/j.scitotenv.2016.07.073>, 2016.

603 Zhang, Y., Tang, L., Croteau, P. L., Favez, O., Sun, Y., Canagaratna, M. R., Wang, Z., Couvidat, F.,  
604 Albinet, A., Zhang, H., Sciare, J., Prévôt, A. S. H., Jayne, J. T., and Worsnop, D. R.: Field  
605 characterization of the PM<sub>2.5</sub> aerosol chemical speciation monitor: insights into the composition,  
606 sources, and processes of fine particles in eastern China, *Atmos. Chem. Phys.*, 17, 14,501–14,517,  
607 <https://doi.org/10.5194/acp-17-14501-2017>, 2017.

608 Zhao, J., Du, W., Zhang, Y., Wang, Q., Chen, C., Xu, W., Han, T., Wang, Y., Fu, P., Wang, Z., Li, Z.,  
609 and Sun, Y.: Insights into aerosol chemistry during the 2015 China Victory Day parade: results from  
610 simultaneous measurements at ground level and 260 m in Beijing, *Atmos. Chem. Phys.*, 17, 3215–  
611 3232, <https://doi.org/10.5194/acp-17-3215-2017>, 2017.

612 Zhong, S., Qian, Y., Sarangi, C., Zhao, C., Leung, R., Wang, H., Yan, H., Yang, T., and Yang, B.:  
613 Urbanization effect on winter haze in the Yangtze River Delta Region of China, *Geophys. Res. Lett.*,  
614 45, 6710–6718, <https://doi.org/10.1029/2018GL077239>, 2018.

615 Zhu, Y., Yan, C., Zhang, R., Wang, Z., Zheng, M., Gao, H., Gao, Y., and Yao, X.: Simultaneous  
616 measurements of new particle formation at 1-s time resolution at a street site and a rooftop site, *Atmos.*  
617 *Chem. Phys.*, 17, 9469–9484, <https://doi.org/10.5194/acp-17-9469-2017>, 2017.

618